Alkyne Activation by Electrophilic $[(\eta\text{-}C_5Me_5)Ru(NO)(R)]^+$ (R = Me, Ph, *p*-Tolyl) Fragments: β-Migratory Insertion, Isomerization, and Metallacycle Formation

Robert M. Burns and John L. Hubbard*

Contribution from the Department of Chemistry and Biochemistry, Utah State University, Logan, Utah 84322-0300

Received May 11, 1994®

Abstract: Treatment of $Cp^*Ru(NO)R_2$ complexes **1-3** with 1 equiv of triflic acid (HOTf) leads to the formation of the triflato complexes $Cp^*Ru(NO)(R)(OTf)$ (**4-6**) (R = CH_3 (**1, 4**), C_6H_5 (**2, 5**), *p*-tolyl (**3, 6**); $Cp^* = \eta^5\text{-}C_5Me_5$). X-ray data for **5** ($C_{17}H_{20}NO_4SF_3Ru$): monoclinic space group $P2_1/n$, a = 10.041(2) Å, b = 13.797(4) Å, c = 15.113(3) Å, β = 106.68(2)°, Z = 4, R/R_w = 4.50/3.37%. The dissociation of the triflate ligands in **4-6** in solution is detectable by NMR spectroscopy. The $\Delta H/\Delta S$ values for equilibrium between bound and free triflate in THF are (−2.1(1) kcal/mol)/(−9(1) eu) for **4** and (−2.3(2) kcal/mol)/(−9(1) eu) for **5**. Triflate dissociation from complexes **4-6** in CH_2Cl_2 is trapped by the binding of PhC≡CPh, leading to the eventual formation of neutral ruthenacyclopentadiene products **8-10** by β-migratory insertion followed by orthometallation of a β-aryl group. X-ray data for **8** ($C_{25}H_{27}NORu$): monoclinic space group $P2_1/c$, a = 16.724(7) Å, b = 7.274(2) Å, c = 17.904(7) Å, β = 102.26(3)°, Z = 4, R/R_w = 4.40/3.89%. X-ray data for **10** ($C_{31}H_{31}NORu$): monoclinic space group $P2_1/n$, a = 9.597(2) Å, b = 22.577(4) Å, c = 12.094(2) Å, β = 101.34(2)°, Z = 4, R/R_w = 4.84/4.57%. Formation of **8** requires a *cis–trans* isomerization in the intermediate σ-vinyl complex formed by methyl β-migratory insertion to the alkyne. A proposed mechanism for the *cis–trans*-σ-vinyl isomerization invokes resonance stabilization through back-donation into the NO-π^* levels of the [Cp*Ru(NO)] fragment. Exclusive formation of **10** when **6** is treated with PhC≡CPh shows orthometallation is rapid in comparison to *cis–trans* isomerization of the intermediate σ-vinyl ligand. Protonation experiments using DOTf show the metallacycle to open first at the Ru–C_{aryl} bond; treatment of **8** with excess HOTf results in the generation of (*E*)-α-methylstilbene and $Cp^*Ru(NO)(OTf)_2$ (**7**).

Introduction

Many studies have shown the importance of metallacyclopentadiene complexes in metal-catalyzed organic chemistry.[1-3] One of the most notable examples is the cyclotrimerization of alkynes catalyzed by so-called "basic" metal complexes such as $CpCo(CO)_2$.[2,4-6] Formation of carbon–oxygen bonds has been observed by coupling of a methyl carboxylate substituent of an iridacyclopentadiene complex with terminal alkynes.[7] The coupling of alkynes and CO mediated by late transition metals has been used as a route to many unsaturated organic derivatives.[1,4]

Electrophilic transition metal complexes are perhaps more often associated with carbon–carbon bond formation in olefin polymerization catalysis.[8-15] However, important information on the assembly of pyridine and arene fragments has been revealed by the formation and reactivity of tantalacyclopentadiene complexes.[16] In analogy to Ziegler–Natta catalysis, the reactions of coordinatively unsaturated [L_nM(alkyl)], [L_nM(aryl)], and [L_nM(hydride)] centers with acetylenes are known, but they are fewer in number compared to studies of olefin insertion reactions.[14,17-24]

* Abstract published in *Advance ACS Abstracts,* September 15, 1994.

(1) Collman, J. P.; Hegedus, L. S.; Norton; J. R. Finke, R. G. *Principles and Applications of Organotransition Metal Chemistry*; University Science Book: Mill Valley, CA, 1987; pp 510–511, 870–872.

(2) (a) Vollhardt, K. P. C. *Acc. Chem. Res.* **1977**, *10*, 1. (b) Vollhardt, K. P. C. *Angew. Chem., Int. Ed. Engl.* **1984**, *23*, 539 and references therein.

(3) McAlister, D. M.; Bercaw, J. E.; Bergman, R. G. *J. Am. Chem. Soc.* **1977**, *99*, 1666.

(4) Schore, N. E. *Chem. Rev.* **1988**, *88*, 1081 and references therein.

(5) (a) Werner, H. *Pure Appl. Chem.* **1982**, *54*, 177. (b) Werner, H.; Lippert, F.; Peters, K.; Vonschnering, H. G. *Chem. Ber.* **1992**, *125*, 347. (c) Werner, H. *Angew. Chem., Int. Ed. Engl.* **1983**, *22*, 927. (d) Werner, H.; Otto, H. *Chem. Ber.* **1986**, *119*, 3866.

(6) (a) Werner, H.; Wolf, J.; Schubert, U.; Ackermann, K. *J. Organomet. Chem.* **1986**, *317*, 327. (b) Werner, H.; Weinand, R.; Knaup, W.; Peters, K.; von Schnering, H. G. *Organometallics* **1991**, *10*, 3967. (c) Werner, H.; Höhn, A. *J. Organomet. Chem.* **1984**, *272*, 105.

(7) (a) O'Connor, J. M.; Pu, L.; Chadha, R. K. *J. Am. Chem. Soc.* **1990**, *112*, 9627. (b) O'Connor, J. M.; Pu, L.; Rheingold, A. L. *J. Am. Chem. Soc.* **1990**, *112*, 9663.

(8) For example see: (a) Dewey, M. A.; Knight, D. A.; Arif, A. M.; Gladysz, J. A. *Z. Naturforsch., B.* **1992**, *47*, 1175. (b) Saura-Llamas, I.; Gladysz, J. A. *J. Am. Chem. Soc.* **1992**, *114*, 2136. (c) Urbanos, F.; Halcrow, M. A.; Fernandez-Baeza, J.; Dahan, F.; Labroue, D.; Chaudret, B. *J. Am. Chem. Soc.* **1993**, *115*, 3484. (d) Rondon, D.; Chaudret, B.; He, X.-D.; Labroue, D. *J. Am. Chem. Soc.* **1991**, *113*, 5671. (e) Honeychuck, R. V.; Bonnesen, P. V.; Farahi, J.; Hersh, W. H. *J. Org. Chem.* **1987**, *52*, 5293. (f) Bonnesen, P. V.; Puckett, C. L.; Honeychuck, R. V.; Hersh, W. H. *J. Am. Chem. Soc.* **1989**, *111*, 6070. (g) Ge, Y.-W.; Sharp, P. R. *Inorg. Chem.* **1993**, *32*, 94. (h) Keady, M. S.; Koola, J. D.; Ontko, A. C.; Merwin, R. K.; Roddick, D. M. *Organometallics* **1992**, *11*, 3417. (i) Schnabel. R. C.; Roddick, D. M. *Inorg. Chem.* **1993**, *32*, 1513. (j) Odenkirk, W.; Rheingold, A. L.; Bosnich, B. *J. Am. Chem. Soc.* **1992**, *114*, 6392. (k) Hollis, T. K.; Robinson, N. P.; Bosnich, B. *J. Am. Chem. Soc.* **1992**, *114*, 5464.

(9) (a) O'Regan, M. B.; Liu, A. H.; Finch, W. C.; Schrock, R. R.; Davis, W. M. *J. Am. Chem. Soc.* **1990**, *112*, 4331. (b) Schrock, R. R.; Kolodziej, R. M.; Liu, A. H.; Davis, W. M.; Vale, M. G. *J. Am. Chem. Soc.* **1990**, *112*, 4338.

(10) For example, see: (a) Jordan, R. F. *Adv. Organomet. Chem.* **1991**, *32*, 325. (b) Jordan, R. F. *J. Chem. Educ.* **1988**, *65*, 285. (c) Borkowsky, S. L.; Baenziger, N. C.; Jordan, R. F. *Organometallics* **1993**, *12*, 486. (d) Crowther, D. J.; Baenziger, N. C.; Jordan, R. F. *J. Am. Chem. Soc.* **1991**, *113*, 1455. (e) Bochmann, M.; Jaggar, A. J.; Nicholls, J. C. *Angew. Chem., Int. Ed. Engl.* **1990**, *29*, 780. (f) Eshuis, J. J. W.; Tan, Y. Y.; Teuben, J. H.; Renkema, J. *J. Mol. Catal.* **1990**, *62*, 277. (g) Waymouth, R.; Pino, P. *J. Am. Chem. Soc.* **1990**, *112*, 4911.

(11) Wang, L.; Flood, T. C. *J. Am. Chem. Soc.* **1992**, *114*, 3169.

(12) (a) Hlatky, G. G.; Turner, H. W.; Eckman, R. R. *J. Am. Chem. Soc.* **1989**, *111*, 2728. (b) Hlatky, G. G.; Eckman, R. R.; Turner, H. W.; *Organometallics* **1992**, *11*, 1413.

(13) (a) Yang, X.; Stern, C. L.; Marks, T. J. *J.Am. Chem. Soc.* **1991**, *113*, 3623. (b) Sishta, C.; Hathorn, R. M.; Marks, T. J. *J. Am. Chem. Soc.* **1992**, *114*, 1112. (c) Marks, T. J. *Acc. Chem. Res.* **1992**, *23*, 57. (d) Yang, X.; Stern, C. L.; Marks, T. J. *Organometallics* **1991**, *10*, 840. (e) Lin, Z.; Le Marechal, J.-F.; Sabat, M.; Marks, T. J. *J. Am. Chem. Soc.* **1987**, *109*, 4127.

(14) Burger, B. J.; Thompson, M. E.; Cotter, W. D.; Bercaw, J. E. *J. Am. Chem. Soc.* **1990**, *112*, 1566.

(15) Hauptman, E.; Brookhart, M.; Fagan, P. J.; Calabrese, J. C. *Organometallics* **1994**, *13*, 774.

(16) Strickler, J. R.; Bruck, M. A.; Wigley, D E. *J. Am. Chem. Soc.* **1990**, *112*, 2814.

(17) Huggins, J. M.; Bergman, R. G. *J. Am. Chem. Soc.* **1981**, *103*, 3002.

0002-7863/94/1516-9514$04.50/0

Table 1. Summary of Crystallographic Data for Complexes **5**, **8**, and **10**

	5	**8**	**10**
empirical formula	$C_{17}H_{20}NF_3O_4RuS$	$C_{25}H_{27}NORu$	$C_{31}H_{31}NORu$
formula weight	492.5	458.5	534.6
crystal system	monoclinic	monoclinic	monoclinic
space group	$P2_1/n$ (no. 14)	$P2_1/c$ (no. 14)	$P2_1/n$ (no. 14)
a (Å)	10.041(2)	16.724(7)	9.597(2)
b (Å)	13.797(4)	7.274(2)	22.577(4)
c (Å)	15.113(3)	17.904(7)	12.094(2)
β (deg)	106.68(2)	102.26(3)	101.34(2)
V (Å^3)	2005.7(8)	2082.0(12)	2569.3(8)
Z	4	4	4
T (°C)	294	173	173
λ (Mo Kα) (Å)	0.710 73	0.710 73	0.710 73
μ (Mo Kα) (mm^{-1})	0.934	0.768	0.633
ρ_{calcd} (g/cm^3)	1.631	1.463	1.382
final R^a (%), $R_w{}^b$ (%)	4.50, 3.37	4.40, 3.89	4.94, 4.57

^{a} $R = \sum||F_o| - |F_c||/\sum|F_o|$. ^{b} $R_w = [\sum w(|F_o| - |F_c|)^2/\sum w|F_o|^2]^{1/2}$; $w = 1/\sigma^2(|F_o|)$.

The recent work of Bercaw and co-workers is a prime case where both olefin and alkyne insertions are compared in the $Cp^*_2ScCH_3$ and Cp^*_2ScH systems.[14]

Following a tradition of generating reactive electrophilic $[L_nM(R)]^+$ centers,[9,11-13d,e,15] we report here the synthesis and characterization of the d^6 complexes Cp*Ru(NO)(R)(OTf) (R = CH_3 (**4**), C_6H_5 (**5**), *p*-tolyl (**6**); OTf = $CF_3SO_3^-$). The dissociation of the triflate ligand leads to the generation of reactive electrophilic $[Cp^*Ru(NO)R]^+$ fragments similar to the $[Cp^*Ru(NO)(Me)(solvent)]^+$ species recently reported by Brookhart and co-workers to activate methyl acrylate.[15] The trapping of the electrophilic $[Cp^*Ru(NO)(R)^+/OTf^-]$ ion pair with PhC≡CPh leads to new ruthenacyclopentadiene complexes, providing a convenient format to evaluate carbon–carbon bond formation, metal–carbon bond formation and cleavage, and intermediate isomerization that leads to the formation of functionalized stilbene byproducts.

Results

Synthesis and Characterization of Complexes 4-6. The treatment of the $Cp^*Ru(NO)R_2$ complexes **1-3** with 1–2 equiv of HOTf gives moderate to good isolated yields of the complexes Cp*Ru(NO)(R)(OTf) (R = CH_3 (**4**), C_6H_5 (**5**), *p*-tolyl (**6**)). The byproduct $Cp^*Ru(NO)(OTf)_2$ (**7**) in these reactions quantitatively accounts for the starting material not converted to complexes **4-6**.[25] The ether-insoluble complex **7** is easily separated from complexes **4-6** by simple extraction techniques. The red-brown triflate complexes **4-6** are very soluble in common polar organic solvents and are somewhat soluble in benzene and toluene.

The single-crystal X-ray diffraction results for complex **5** are summarized in Tables 1–3. Figure 1 shows the molecule to possess a three-legged piano stool geometry with the Cp* ring symmetrically bound to the Ru atom (average Ru–Cp* length 2.235(7) Å). The Ru–N–O(1) bond angle is 172.3(6)° with a Ru–OTf bond distance of 2.146(4) Å and a Ru–C(21) (*ipso*-C_6H_5) bond length of 2.100(5) Å.

The electron impact (EI) mass spectra of complexes **4-6** all show low-intensity (4–5%) molecular ions relative to a base peak of $[Cp^*]^+$. Other major fragments observed include $[Cp^*Ru(NO)(OTf)]^+$ and $[Cp^*Ru(OTf)]^+$. The IR spectra for **4-6** in CH_2Cl_2 show ν_{NO} values between 1780 and 1800 cm^{-1}, consistent with linear nitrosyl coordination. The ^{1}H NMR spectrum shows the Cp* resonances at δ 1.77 (**4**) and δ 1.72 (**5** and **6**).

The ^{19}F NMR spectra of complexes **4** and **5** in $CDCl_3$ or CH_2Cl_2 exhibit a single resonance at δ −76.5. In pure THF the ^{19}F NMR spectra of **4** and **5** show two resonances whose intensities are temperature dependent (vide infra). The IR spectra of **4-6** in THF show only one distinct ν_{NO} absorption.

Reactivity of Complex 1 with PhC≡CPh. Addition of 10 equiv of PhC≡CPh to a $CDCl_3$ solution of **4** leads to the appearance of a new signal at δ −77.7 in the ^{19}F NMR spectrum. Monitoring the reaction by ^{19}F NMR spectroscopy shows the intensity of this new resonance to be 22% of the total ^{19}F signal after 1 h, 94% after 14 h, and 100% after 30 h. The rate of disappearance of

Table 2. Selected Geometric Data for **5**

Bond Lengths (Å)			
Ru–N	1.758(5)	N–O(1)	1.145(7)
Ru–O(2)	2.146(4)	Ru–C(4)	2.186(8)
Ru–C(1)	2.202(6)	Ru–C(5)	2.211(6)
Ru–C(2)	2.291(6)	Ru–C(21)	2.100(5)
Ru–C(3)	2.289(7)		
Bond Angles (deg)			
Ru–N–O(1)	172.3(6)	O(2)–Ru–C(21)	86.5(2)
O(2)–Ru–N	100.7(2)	N–Ru–C(21)	91.5(2)

Table 3. Atomic Coordinates (×10^4) and Equivalent Isotropic Displacement Coefficients (Å^2 × 10^3) for **5**

	x	y	z	$U_{eq}{}^a$
Ru	4996(1)	1729(1)	1595(1)	36(1)
S	7142(2)	2299(1)	392(1)	50(1)
O(2)	6649(4)	2440(3)	1211(2)	45(2)
O(3)	7800(5)	3148(3)	175(3)	83(2)
O(4)	6205(4)	1786(4)	−344(3)	69(2)
C(6)	8585(8)	1479(6)	802(6)	66(3)
F(1)	9116(5)	1218(4)	149(3)	132(3)
F(2)	8207(5)	690(3)	1176(3)	92(2)
F(3)	9576(4)	1880(4)	1488(3)	113(2)
N	4238(5)	1053(4)	590(4)	51(2)
O(1)	3625(6)	592(4)	−21(4)	103(3)
C(1)	5450(7)	2221(5)	3037(4)	48(3)
C(2)	6480(7)	1518(7)	3048(4)	62(3)
C(3)	5817(9)	633(6)	2761(5)	67(4)
C(4)	4357(8)	794(5)	2567(4)	57(3)
C(5)	4155(6)	1766(6)	2795(3)	47(2)
C(11)	5732(8)	3238(5)	3375(4)	97(4)
C(12)	8024(7)	1691(7)	3339(4)	118(4)
C(13)	6486(11)	−322(6)	2699(6)	157(7)
C(14)	3255(9)	33(6)	2290(5)	126(5)
C(15)	2810(7)	2193(6)	2862(5)	92(4)
C(22)	4328(6)	3860(5)	1010(4)	44(2)
C(23)	3500(7)	4640(5)	653(4)	54(3)
C(25)	2077(7)	4523(5)	321(4)	57(3)
C(24)	1504(7)	3628(5)	348(4)	52(3)
C(26)	2328(6)	2852(4)	708(4)	40(2)
C(21)	3776(6)	2944(4)	1051(3)	34(2)

^{a} Equivalent isotropic U defined as one-third of the trace of the orthogonalized U_{ij} tensor: $U_{eq} = {}^1/_3\sum_i\sum_j U_{ij}a_i^*a_j^*a_ia_j$.

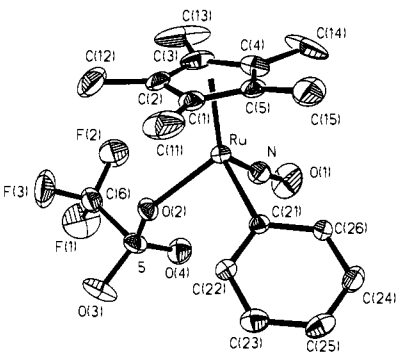

Figure 1. Thermal ellipsoid plot (30% probability level) and atom numbering scheme for complex **5**.

(18) Chisholm, M. H.; Clark, H. C. *Inorg. Chem.* **1971**, *10*, 2557.
(19) Stack, J. G.; Simpson, R. D.; Hollander, F. J.; Bergman, R. G.; Heathcock, C. H. *J. Am. Chem. Soc.* **1990**, *112*, 2716, and references therein.
(20) Horton, A. D.; Orpen, A. G. *Organometallics* **1991**, *10*, 3910.
(21) Evitt, E. R.; Bergman, R. G. *J. Am. Chem. Soc.* **1980**, *102*, 7003.
(22) Guram, A. S.; Guo, Z.; Jordan, R. F. *J. Am. Chem. Soc.* **1993**, *115*, 4902.
(23) Villanueva, L. A.; Abboud, K. A.; Boncella, J. M. *Organometallics* **1992**, *11*, 2963.
(24) Samsel, E. G.; Norton, J. R. *J. Am. Chem. Soc.* **1984**, *106*, 5505.
(25) (a) Zoch, C. R. Dissertation, Utah State University, 1993. (b) Hubbard, J. L.; Zoch, C. R. Manuscript in preparation.

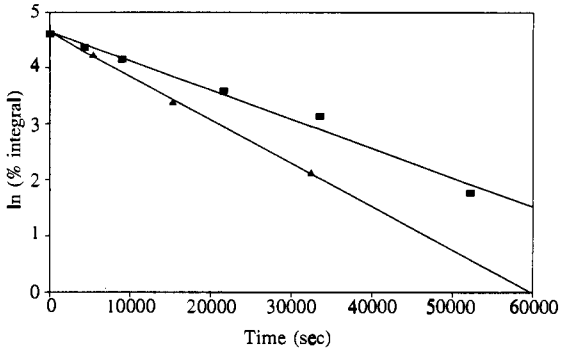

Figure 2. ln(% integral) versus time for the ^{19}F NMR spectroscopy of complexes **4** (■) and **5** (▲).

Table 4. Selected Geometric Data for **8** and **10**

Bond Lengths (Å)			
complex **8**		complex **10**	
Ru–N(1)	1.743(5)	Ru–N	1.747(6)
N(1)–O(1)	1.187(6)	N–O	1.172(8)
Ru–Cp* (av)	2.30(1)	Ru–Cp* (av)	2.27(1)
Ru–C(8)	2.129(5)	Ru–C(7)	2.114(7)
Ru–C(45)	2.093(5)	Ru–C(42)	2.088(8)
C(6)–C(8)	1.351(7)	C(6)–C(7)	1.359(11)
C(6)–C(46)	1.473(7)	C(6)–C(41)	1.472(12)
C(41)–C(42)	1.405(7)	C(41)–C(42)	1.400(10)
C(41)–C(46)	1.408(7)	C(41)–C(46)	1.402(11)
C(42)–C(43)	1.393(9)	C(42)–C(43)	1.391(12)
C(43)–C(44)	1.401(8)	C(43)–C(44)	1.413(12)
C(44)–C(45)	1.398(7)	C(44)–C(45)	1.368(12)
C(45)–C(46)	1.422(8)	C(45)–C(46)	1.379(12)
Bond Angles (deg)			
complex **8**		complex **10**	
Ru–N(1)–O(1)	177.4(4)	Ru–N–O	174.5(6)
N(1)–Ru–C(8)	94.5(2)	N–Ru–C(7)	98.2(3)
N(1)–Ru–C(45)	96.7(2)	N–Ru–C(42)	95.2(3)
C(8)–Ru–C(45)	77.1(2)	C(7)–Ru–C(42)	78.0(3)
C(8)–C(6)–C(46)	113.8(5)	C(7)–C(6)–C(41)	115.1(7)
Ru–C(8)–C(6)	117.9(3)	Ru–C(7)–C(6)	116.2(6)
Ru–C(45)–C(46)	115.3(3)	C(6)–C(41)–C(42)	115.2(7)
C(6)–C(46)–C(45)	115.5(4)	Ru–C(42)–C(41)	115.4(6)

complex **4** under these pseudo-first-order conditions gives k_{obs} = 4.1(9) × 10^{-5} s^{-1}, compared to k_{obs} = 7.7(2) × 10^{-5} s^{-1} for the disappearance of complex **5** (Figure 2). Monitoring the same reaction by ^1H NMR spectroscopy shows transient resonances at δ 1.64 and δ 1.35 that appear within one h and are absent after 30 h. Monitoring a reaction with a 1:1 mixture of complex **4** and PhC≡CPh shows ^1H NMR signals at δ 2.45 and other transient resonances between δ 1.66 and δ 1.80. The appearance of (*Z*)-α-methylstilbene together with $Cp^*Ru(NO)(OTf)_2$ is also observed by ^1H NMR spectroscopy in the reaction mixtures of **4** with PhC≡CPh.[26] The production of (*Z*)-α-methylstilbene is not observed when 2 equiv of the base *N*,*N*-diisobutyl-2,4-dimethyl-3-pentylamine is present in solution.

Characteristics of Ruthenacyclopentadiene Complexes 8-10. Crystals of the orange, air-stable ruthenacyclopentadiene complexes **8-10** are isolated from the crude reaction mixtures of **4-6** and PhC≡CPh by simple recrystallization from hexane. The X-ray structures of complexes **8** and **10** are shown in Figures 3 and 4, and the crystallographic data are summarized in Tables 1 and 4–6. The molecules show symmetrically bound Cp* ligands and nearly linear nitrosyl coordination. For both **8** and **10** the data reveal a metallacyclopentadiene core, with an alternating long–short–long–short–long pattern around the RuC=CC=C ring. The Ru atoms deviate from a plane containing the carbon skeleton by 0.18 Å for **8** and 0.08 Å for **6**. The phenyl substituents attached to the metallacycle rings lie between 45° and 65° out of the plane of the metallacycle.

(26) Kawashima, T.; Ishii, T.; Inamoto, N. *Bull. Chem. Soc. Jpn.* **1987**, *60*, 1831. ^1H NMR ($CDCl_3$): (*Z*)-α-methylstilbene, δ 2.19 (d, 3H, *J* = 1.5 Hz), δ 6.46 (br, 1H); (*E*)-α-methylstilbene, δ 2.26 (d, 3H, *J* = 1.2 Hz), δ 6.83 (br, 1H).

Table 5. Atomic Coordinates (×10^5) and Equivalent Isotropic Displacement Coefficients (Å² × 10^3) for **8**

	x	*y*	*z*	U_{eq}[a]
Ru	27 066(3)	11 567(6)	21 005(2)	158(1)
N(1)	32 495(28)	31 858(66)	20 586(25)	191(16)
O(1)	36 461(25)	45 335(58)	20 459(23)	334(15)
C(1)	21 674(33)	−16 732(72)	16 376(32)	223(19)
C(2)	25 183(33)	−18 584(73)	24 350(32)	213(19)
C(3)	33 775(32)	−14 926(72)	25 446(31)	205(19)
C(4)	35 499(32)	−10 318(82)	18 140(30)	229(18)
C(5)	28 043(32)	−11 528(86)	12 495(28)	243(17)
C(11)	13 027(36)	−21 599(91)	12 720(38)	423(25)
C(12)	20 822(39)	−25 993(86)	30 296(34)	388(25)
C(13)	39 932(37)	−17 677(86)	32 828(34)	385(23)
C(14)	43 920(36)	−7 160(92)	16 434(39)	436(27)
C(15)	27 252(41)	−9 271(93)	3 866(29)	395(23)
C(7)	10 454(33)	32 973(80)	35 776(29)	251(20)
C(6)	14 843(31)	26 083(72)	29 669(28)	177(18)
C(8)	22 584(33)	19 655(73)	30 785(26)	181(17)
C(31)	36 278(34)	25 406(83)	39 595(31)	258(20)
C(32)	41 605(35)	23 385(92)	46 687(32)	337(22)
C(33)	39 159(36)	14 333(94)	52 658(32)	365(23)
C(34)	31 270(37)	7 456(79)	51 726(31)	306(22)
C(35)	25 853(33)	9 147(81)	44 594(28)	242(19)
C(36)	28 233(32)	18 352(72)	38 431(29)	188(18)
C(41)	2 564(32)	33 304(73)	18 944(31)	239(19)
C(42)	−675(34)	34 102(77)	11 041(32)	289(21)
C(43)	4 153(34)	29 669(82)	5 841(31)	272(20)
C(44)	12 223(34)	23 612(79)	8 382(30)	255(20)
C(45)	15 476(33)	22 162(73)	16 224(29)	191(18)
C(46)	10 665(31)	27 183(74)	21 566(29)	177(18)

[a] Equivalent isotropic *U* defined as one-third of the trace of the orthogonalized U_{ij} tensor: $U_{eq} = {}^1/_3\sum_i\sum_j U_{ij}a_i^*a_j^*a_ia_j$.

Table 6. Atomic Coordinates (×10^4) and Equivalent Isotropic Displacement Coefficients (Å² × 10^3) for **10**

	x	*y*	*z*	U_{eq}[a]
Ru	451(1)	1928(1)	1631(1)	20(1)
N	1451(7)	2518(3)	2305(5)	22(2)
O	2020(6)	2940(3)	2745(5)	41(2)
C(1)	−855(9)	1390(4)	204(8)	38(4)
C(2)	−395(8)	1904(6)	−268(6)	42(3)
C(3)	−999(10)	2392(4)	208(7)	32(3)
C(4)	−1857(9)	2169(4)	957(7)	33(3)
C(5)	−1761(9)	1545(4)	941(7)	32(3)
C(11)	−590(10)	754(4)	−118(9)	75(5)
C(12)	444(9)	1932(6)	−1188(6)	81(5)
C(13)	−878(10)	3029(4)	−100(8)	67(4)
C(14)	−2760(11)	2549(5)	1563(8)	72(5)
C(15)	−2586(10)	1127(5)	1508(9)	72(5)
C(6)	2271(8)	918(3)	2613(6)	21(3)
C(7)	2112(8)	1303(3)	1734(6)	20(3)
C(22)	3164(5)	762(2)	295(4)	26(2)
C(23)	3934	758	−570	37(2)
C(24)	4547	1280	−867	37(2)
C(25)	4390	1806	−298	34(2)
C(26)	3619	1810	567	29(2)
C(21)	3006	1288	864	22(2)
C(41)	1279(8)	1003(3)	3385(6)	21(3)
C(42)	329(8)	1476(3)	3115(6)	23(3)
C(43)	−593(8)	1618(3)	3831(7)	28(3)
C(44)	−614(9)	1282(4)	4813(7)	33(3)
C(45)	309(9)	816(4)	5045(7)	36(3)
C(46)	1253(8)	673(3)	4363(6)	27(3)
C(32)	4848(5)	645(2)	3165(4)	28(2)
C(33)	5925	225	3445	36(2)
C(34)	5586	−375	3452	34(2)
C(35)	4169	−556	3180	29(2)
C(36)	3092	−135	2900	27(2)
C(31)	3431	465	2892	20(2)
C(54)	−1658(10)	1429(4)	5558(7)	43(4)

[a] Equivalent isotropic *U* defined as one-third of the trace of the orthogonalized U_{ij} tensor: $U_{eq} = {}^1/_3\sum_i\sum_j U_{ij}a_i^*a_j^*a_ia_j$.

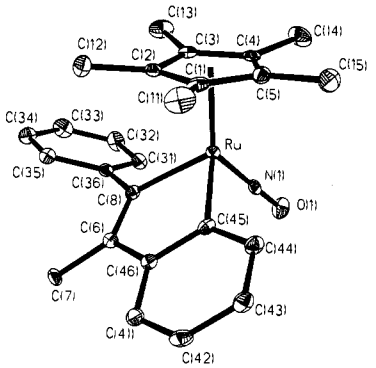

Figure 3. Thermal ellipsoid plot (30% probability level) and atom numbering scheme for complex **8**.

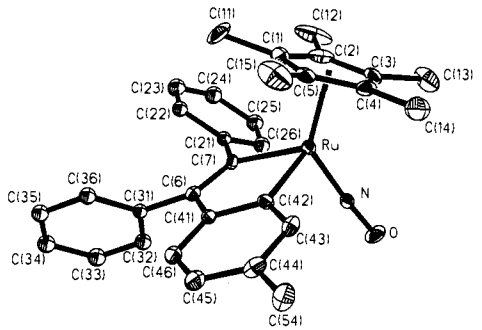

Figure 4. Thermal ellipsoid plot (30% probability level) and atom numbering scheme for complex **10**.

Complex **8** shows a pair of resonances at δ 1.52 and δ 2.12 in a 15:3 intensity ratio consistent with their assignment as the Cp* and CH_3 resonances, respectively. Complexes **9** and **10** show similar Cp* resonances, and **10** shows a singlet at δ 2.30 characteristic of the *p*-tolyl CH_3 group. Also observed for complexes **8–10** are resonances attributable to aromatic protons between δ 6.7 and δ 7.6. The complexes display strong ν_{NO} absorptions at 1738, 1734, and 1736 cm^{-1} for **8–10**, respectively. The mass spectra of complexes **8–10** all show a relatively intense molecular ion, with the base peak being loss of the NO ligand in each case.

Treatment of Complex 8 with HOTf. Treatment of **8** with excess HOTf leads to the quantitative formation of complex **7** and (*E*)-α-methylstilbene by ^1H NMR spectroscopy. As examined by ^1H NMR spectroscopy, treatment of pure complex **8** with 1 equiv of HOTf in $CDCl_3$ leads to a color change from orange to yellow-brown and the appearance of new signals at δ 1.79 and δ 2.52 together with signals attributable to complex **7**. Infrared analysis of a similar reaction shows a new ν_{NO} at 1783 cm^{-1} together with absorptions from complexes **8** and **7**.

Treatment of **8** with 0.5 equiv of HOTf in $CDCl_3$ leads to the generation of resonances at δ 1.79 and δ 2.52 in the ^1H NMR spectrum. After 12 h these resonances are replaced by resonances for complex **7** and (*E*)-α-methylstilbene and the reappearance of intensity in the resonances due to **8**. Treatment of **8** with 0.5 equiv of DOTf produces a single resonance at δ 7.10 in the ^2H NMR spectrum. Subsequent addition of excess DOTf leads to a second signal in the ^2H NMR spectrum at δ 6.9.

Discussion

Preparation of Triflato Complexes 4-6. Treatment of the dialkyl complexes with 1 equiv of HOTf produces the Cp*Ru(NO)(R)(OTf) derivatives **4-6** together with significant amounts of $Cp^*Ru(NO)(OTf)_2$ (**7**) in an essentially quantitative combined yield (eqs 1 and 2). The ditriflato complex is produced

$$\underset{\textbf{1-3}}{Cp^*Ru(NO)R_2} + HOTf \rightarrow \underset{\textbf{4-6}}{Cp^*Ru(NO)(R)(OTf)} + RH \quad (1)$$

$$\underset{\textbf{4-6}}{Cp^*Ru(NO)(R)(OTf)} + HOTf \rightarrow \underset{\textbf{7}}{Cp^*Ru(NO)(OTf)_2} + RH \quad (2)$$

$$R = CH_3,\ C_6H_5,\ p\text{-}C_6H_4CH_3$$

even when a substoichiometric amount of HOTf is added, indicating that the protonation of $Cp^*Ru(NO)(R)_2$ is not as facile as the protonation of the Cp*Ru(NO)(R)(OTf) complexes **4-6**. This is particularly the case when R = Ph or *p*-tolyl. In comparison, the reactions of complexes **1** and **2** with aqueous HCl reported by Bergman and co-workers show that the Cp*Ru(NO)(R)(Cl) products are somewhat resistant to further reaction to give $Cp^*Ru(NO)Cl_2$.[27]

The X-ray structure of complex **5** shows a bound triflate ligand. In comparison to Ru–triflato complexes reported by Wojcicki *et al.*,[28] complex **5** has a Ru–O bond that is the same as that reported for $[Cp^*Ru(NO)(CH(CH_3)COOCH_3)]^+$. These Ru–O distances are more characteristic of Ru–O bond distances found for better anionic oxygen donors such as tosylate, trifluoroacetate, and benzoate (Table 7).[29-31] The shortness of the Ru–OTf bond in complex **5** supports the more electrophilic nature of the $[Cp^*Ru(NO)R]^+$ fragment in comparison to the $[(Cyttp)Ru^{II}(CO)]^{2+}$ fragment.

The modest, but significant solubility of complexes **4-6** in benzene and toluene is a strong indication that the complexes dissolve without dissociation of the triflate ligand. The ^{19}F NMR spectra of **4-6** in toluene-d_8, $CDCl_3$, or CH_2Cl_2 show only one fluorine resonance, lending strong spectral evidence for the presence of a single triflate environment. The mass spectra of complexes **4-6** show the triflate ligands to be tightly bound to the metal, producing molecular ions of ca. 5% relative intensity together as well as a number of more intense fragments like $[Cp^*Ru(OTf)]^+$ and $[Cp^*Ru(NO)(OTf)]^+$. The IR data for complexes **4-6** show a single ν_{NO} absorption for each complex. The ν_{NO} absorption for the methyl complex **4** is ca. 10 cm^{-1} lower than the aryl derivatives **5** and **6**, consistent with the stronger donor character of a CH_3 ligand.

Dissociation of the Triflate Ligand. It is evident by ^{19}F NMR spectroscopy that triflate dissociation occurs when complexes **4-6** are dissolved in THF. A resonance at δ −77.5 coincides where added free OTf^- is observed, and a second resonance at δ −76.5 is attributed to a bound OTf^- ligand. The equilibrium constants (22 °C) for the solvolysis reactions shown in eqs 3 and 4 are 0.02 and 0.11, respectively. The temperature dependence of these equilibria is shown in Figure 5. The van't Hoff analysis in THF

$$\underset{\textbf{4}}{Cp^*Ru(NO)(CH_3)(OTf)} + THF_{(l)} \rightleftarrows \underset{\textbf{4a}}{[Cp^*Ru(NO)(CH_3)(THF)]^+} + OTf^- \quad K_{eq} = 0.02 \quad (3)$$

$$\underset{\textbf{5}}{Cp^*Ru(NO)(Ph)(OTf)} + THF_{(l)} \rightleftarrows \underset{\textbf{5a}}{[Cp^*Ru(NO)(Ph)(THF)]^+} + OTf^- \quad K_{eq} = 0.11 \quad (4)$$

gives $\Delta H = -2.1(3)$ kcal/mol and $\Delta S = -9(1)$ eu for complex **4** and $\Delta H = -2.3(2)$ kcal/mol and $\Delta S = -9(1)$ eu for complex **5**.

(27) The Cp*Ru(NO)(Ph)Cl derivative is apparently more sensitive to $HCl_{(aq)}$ than the Cp*Ru(NO)(Me)(Cl) complex: (a) Chang. J.; Bergman, R. G. *J. Am. Chem. Soc.* **1987**, *109*, 4298. (b) Chang. J.; Seidler, M. D.; Bergman, R. G. *J. Am. Chem. Soc.* **1989**, *111*, 3258.

(28) Blosser, P. W.; Gallucci, J. C.; Wojcicki, A. *Inorg. Chem.* **1992**, *31*, 2376.

(29) Rotem, M.; Stein, Z.; Shvo, Y. *J. Organomet. Chem.* **1990**, *387*, 95.

(30) Albers, M. O.; Liles, D. C.; Singleton, E. *Acta Crystallogr., C* **1987**, *43*, 860.

(31) Harding, P. A.; Robinson, S. D.; Henrick, K. *J. Chem. Soc., Dalton Trans.* **1988**, 415.

Table 7. Ru–O Bond Lengths of Selected Ru^{II} Complexes

bond	length (esd) (Å)	complex	ref
Ru–OTf	2.146(4)	Cp*Ru(NO)(Ph)(OTf) (**5**)	this work
Ru–OTf	2.233(3)	*cis*-$Ru(OTf)_2(CO)(Cyttp)^a$	28
	2.221(3)		
Ru–OC(O)Ph	2.083(7)	$Ru(CO)_2(PPh_3)_2(OOCPh)_2$	29
	2.086(7)		
$Ru–OC(O)CF_3$	2.158(4)	$Ru(H_2O)(PMe_3)_3(OOCCF_3)_2$	30
	2.179(4)		
$Ru–OTs^b$	2.162(6)	$Ru(H_2O)(CO)(PPh_3)_2(OTs)_2$	31
	2.165(5)		

^{a} Cyttp = $(PhP(CH_2CH_2CH_2PCy_2)_2)$. ^{b} OTs = $OSO_2C_6H_4$-*p*-CH_3.

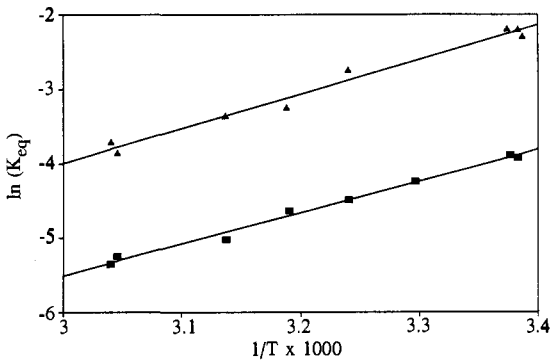

Figure 5. $\ln(K_{eq})$ versus $1/T$ for complexes **4** (■) and **5** (▲).

The ΔS values obtained indicate that neutral triflate complexes **4-6** are favored over the $[Cp^*Ru(NO)(R)(THF)]^+/[OTf]^-$ ion pairs **4a–6a** at high temperatures. This is likely due to the entropic penalty for solvent organization required for the formation and stabilization of the ion pair. The similar ΔH values for the two reactions indicate relatively little substituent effect between R = CH_3 and R = Ph.

It is perhaps surprising that the equilibria depicted in eqs 3 and 4 are not readily detected in the THF solution IR spectra of complexes **4-6**. The formation of cationic derivatives from neutral precursors most often leads to ν_{NO} absorptions at higher energy. Since the NMR data obviously reveal the equilibrium processes depicted in eqs 3 and 4, we deduce that the ν_{NO} absorption of the cationic $[Cp^*Ru(NO)(R)(THF)]^+$ species is coincident with that of the parent Cp*Ru(NO)(R)(OTf) complex. A possible explanation for this could be an increase in π-donation to the metal center by the THF ligand, leading to a significant reduction of the ν_{NO} absorption energy for the cationic complex. Strong π-withdrawing power anticipated for the adjacent $-SO_2CF_3$ moiety in the OTf^- case may reduce the π-donor ability of OTf^-, limiting its interaction with the metal to one of primarily σ-donor character.

Formation and Structure of Ruthenacyclopentadiene Complexes. The treatment of complexes **4-6** with PhC≡CPh in CD_2Cl_2 leads to formation of metallacycle complexes **8-10** over a period of 30 h at ambient temperature. The presence of a small amount of (*Z*)-α-methylstilbene is apparent in the ^1H NMR spectra of the crude reaction mixtures. Since the reaction shown in eq 5 requires

$$\underset{\textbf{4-6}}{Cp^*Ru(NO)(R)(OTf)} + PhC{\equiv}CPh \rightarrow \underset{\textbf{8-10}}{Cp^*(NO)Ru(C(Ph){=}C(R)C_6H_3R')} + HOTf \quad (5)$$

the production of 1 equiv of HOTf, the hindered base *N,N*-diisobutyl-2,4-dimethyl-3-pentylamine was added to consume the HOTf. Under these conditions, an increased yield of metallacycle products **8-10** is obtained and no (*Z*)-stilbene byproduct is observed (vide infra).

The essential X-ray structural features of complexes **8** and **10** (Figures 3 and 4) are very similar. In both cases, it is clear that the migrating CH_3 or *p*-tolyl groups end up exclusively on a β-site

Scheme 1

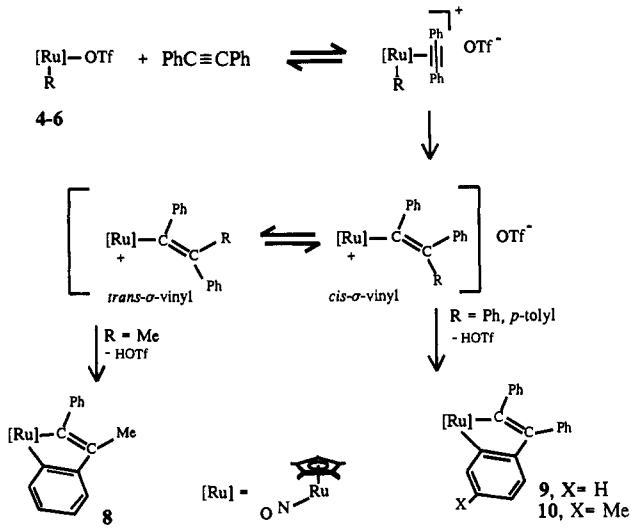

of the metallacycle ring. The Ru–C_{aryl} and Ru–C_{vinyl} bond distances are typical of those found in other Ru^{II} complexes.[32] The Ru–C_{aryl} distance in the metallacyclopentatriene complex reported by Singleton *et al.* (1.942(6) Å) is much shorter than that found in complexes **8** and **10**.[33] The alternating bond lengths about the metallacycle ring are characteristic of metallacyclic complexes containing $[CpRh(PR_3)]$, $[CpIr(PR_3)]$, and $[(\eta\text{-}C_6H_6)Os(PR_3)]$ moieties reported by Werner.[6] Although the X-ray data show the Ru–N–O angle in complex **8** to be ca. 3° larger than that in complex **10**, the ν_{NO} absorptions of **8-10** do not show a significant electronic substituent effect. In fact, the differences in Ru–N and N–O distances (which are often a better gauge to assess a change in metal→NO back-donation) are not significant between complexes **8** and **10**.

Proposed Mechanism for the Formation of Complexes 8-10. The reaction of complexes **4-6** with PhC≡CPh likely follows a pathway that initiates with the dissociation of a triflate ligand from the parent complexes (Scheme 1). Monitoring the reaction of **4** and **5** with a 10-fold excess of PhC≡CPh by ^{19}F NMR spectroscopy shows the steady increase of the concentration of free OTf^- as a function of time, leading to pseudo-first-order rate constants $5.2(3) \times 10^{-5}$ s^{-1} and $7.7(2) \times 10^{-5}$ s^{-1} for the disappearance of complexes **4** and **5**, respectively. Monitoring a similar reaction of complex **4** with PhC≡CPh by ^1H spectroscopy over a similar time period shows transient singlet resonances at δ 1.64 and δ 1.35 that may be tentatively assigned as evidence for a transient $[Cp^*Ru(NO(CH_3)(PhC{\equiv}CPh)]^+$ complex. The observation of a later transient singlet resonance at δ 2.45 may be due to the methyl group of the σ-vinyl complex; however, a separate Cp* resonance is not readily identifiable. Thus, it is not possible to establish the efficiency of β-migratory insertion under the conditions of this reaction. It is unlikely that reversible β-migratory insertion occurs in these systems. Even though the kinetic data show that the phenyl complex **5** disappears faster than complex **4**, to argue that the migratory aptitude for Ph is greater than CH_3 is in serious conflict with work by previous researchers.[14] In correlation with the equilibrium observed in THF (eqs 3 and 4), it is possible that the solvolysis of OTf^- in CH_2Cl_2 is more favorable for complex **5**, making the trapping of the $[Cp^*Ru(NO)(Ph)]^+$ species more efficient than the trapping of the $[Cp^*Ru(NO)(Me)]^+$ species.

In the reaction of complex **4** with PhC≡CPh to give metallacycle **8**, it is readily apparent that the regiochemistry of complex **8** is not attainable from an intermediate σ-vinyl complex without a *cis–trans* isomerization about the double bond of the

(32) Bruce, M. I.; Koutsantonis, G. A.; Liddell, M. J.; Tiekink, E. R. T. *J. Organomet. Chem.* **1991**, *420*, 253.
(33) Albers, M. O.; de Waal, D. J. A.; Liles, D. C.; Robinson, D. J.; Singleton, E.; Wiege, M. B. *J. Chem. Soc., Chem. Commun.* **1986**, 1680.

[RuC(Ph)=CPh(Me)] moiety (Scheme 1). The kinetic product of insertion is expected to be a *cis*-σ-vinyl intermediate. The observation of small amounts of (*Z*)-α-methylstilbene in the reaction mixtures is consistent with some loss of the σ-vinyl ligand before isomerization occurs. The HOTf required for this cleavage step is presumably produced as the byproduct from the final step of orthometalation.

Since the reaction of complex **5** with PhC≡CPh leads to a σ-vinyl intermediate that possesses two β-phenyl groups, isomerization is not required to give the metallacycle product **9**. However, in the reaction of complex **6** with PhC≡CPh, only the formation of complex **10** is observed. This indicates that *cis–trans* isomerization of the σ-vinyl intermediate is slow compared to orthometalation.

It is possible to rationalize the *cis–trans* isomerization by invoking the resonance structure **A**, where the Ru fragment formally attains a d^8 configuration similar to that found for several Cp*Ru(NO)(L) complexes described by Bergman and coworkers.[27] The tertiary carbonium ion is localized on the β-carbon atom that has a phenyl group and is stabilized by the triflate counterion.

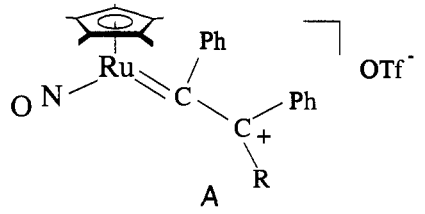

A

Werner[6b] and Bergman[17] have independently observed *cis–trans* isomerization of σ-vinyl ligands, invoking a resonance form similar to that of **A**. A similar isomerization is also quite likely involved in the formation of σ-vinyl products reported by Mawby et al.[34] Horton and Orpen's[20] recent report of zirconocene-type σ-vinyl complexes described two isomers that are presumably *cis–trans*-σ-vinyl intermediates. Very recently, Alper[35] discussed the appearance of both *cis* and *trans* isomers of the products following alkyne addition to a Pd center. The proposed mechanism of isomerization in these Pd complexes also involves a resonance form B where a d^8 Pd center formally donates an electron pair to form the M=C bond, generating a zwitterionic $Pd^+=C-C^-$ resonance structure.

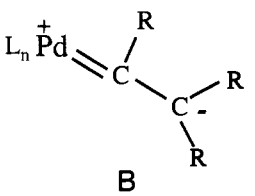

B

Reactivity of Metallacycle 8 with HOTf. As monitored by ^1H NMR spectroscopy, the treatment of purified complex **8** with 1 equiv of HOTf leads to the observation of signals at δ 1.79 and δ 2.52. These signals are similar to those of transient species observed in the reactions leading to the formation of complex **8** (*vide supra*) and are taken as evidence that the metallacycle ring can be opened in a stepwise fashion. Monitoring the treatment of metallacycle complex **8** with less than 1 equiv of DOTf by ^2H NMR spectroscopy shows the appearance of one signal at δ 7.2, consistent with the cleavage of the Ru–C_{aryl} bond and the appearance of an aryl-type ^2H resonance. Continued addition of DOTf leads to the observation of a second resonance at δ 6.9 characteristic of a vinyl proton of (*E*)-α-methylstilbene. This evidence shows the Ru–C_{aryl} bond is more readily attacked by D^+ than is the Ru–C_{vinyl} bond.

(34) Crook, J. R.; Chamberlin, B.; Mawby, R. J. *J. Chem. Soc., Dalton Trans.* **1989**, 465.
(35) Zargarian, D.; Alper, H. *Organometallics* **1993**, *12*, 712.

Treatment of purified metallacycle complex **8** with excess HOTf leads to the clean generation of Cp*Ru(NO)$(OTf)_2$ and (*E*)-α-methylstilbene. The fact that no (*Z*)-α-methylstilbene is detected shows that isomerization in the σ-vinyl intermediate is not a significant process under these conditions.

Summary

We have shown that triflate dissociation from Cp*Ru(NO)(R)(OTf) complexes leads to the formation of electrophilic [Cp*Ru(NO)(R)]+ fragments that can bind and activate PhC≡CPh. The final metallacyclic products are observed after a series of intermediate steps including β-migratory insertion and *cis–trans* isomerization of a transient Ru–σ-vinyl species. Throughout this series of events, it is important to consider the OTf^- species both as a competitive ligand and as a stabilizing factor for intermediates that are formed after β-migratory insertion. The successive addition of more PhC≡CPh units to an intermediate Ru–σ-vinyl species is likely impeded by the presence of OTf^-. Facilitation of the *cis–trans* isomerization required for the formation of complex **8** is very likely the result of a favorable π-resonance interaction from the vinyl group into the strongly π-accepting [Cp*Ru(NO)] fragment coupled with the action of OTf^- to help stabilize the positive charge on the terminal carbon atom. Work concerning the reactivity of unsaturated organic species with triflate-free [Cp*Ru(NO)(R)(THF)]+ cations is the subject of forthcoming reports from our laboratory.

Experimental Section

General Procedures. All manipulations were carried out under Schlenk techniques. The nitrogen atmosphere was purified by passing it through scavengers for water (Aquasorb, Mallinckrodt) and oxygen (Catalyst R3-11, Chemical Dynamics, South Plainfield, NJ). All solvents were distilled under nitrogen over appropriate drying agents prior to use. Chemical reagents were used as received from Aldrich unless stated otherwise. Complexes **1-3** were prepared by literature methods.[27,36] *N,N*-Diisobutyl-2,4-dimethyl-3-pentylamine (Fluka) was distilled from CaH_2 and stored under N_2 until use. Infrared spectra were recorded on a Mattson Polaris-Icon FT spectrophotometer. The ^1H, ^{13}C, and ^{19}F NMR spectra were recorded on a Varian XL300 spectrometer operating at 300 MHz (^1H), 282 MHz (^{19}F), and 46.0 MHz (^2H) and a JEOL GX270 spectrometer operating at 270 MHz (^1H) and 68.9 MHz (^{13}C). Residual solvent peaks were used as internal standards (δ 5.32 (^1H) and δ 53.8 (^{13}C) for CD_2Cl_2; δ 7.24 (^1H) and δ 77.0 (^{13}C) for $CDCl_3$). ^{19}F NMR chemical shifts are reported with respect to an external trifluoroacetic acid standard (δ −76.53) upfield of $CFCl_3$ (δ 0). ^2H NMR shifts are reported with respect to an external $CDCl_3$ resonance (δ 7.24). Mass spectra were obtained on a LKB 2091 mass spectrometer using electron impact ionization and a heated direct inlet probe. Melting points were measured with a Mel-Temp device (Laboratory Devices) in open capillaries and are uncorrected. Combustion analyses were performed by Atlantic Microlab, Inc., Norcross, GA.

Synthesis of Cp*Ru(NO)(CH_3)(OTf) (4). To a stirred solution (CH_2Cl_2, 40 mL) of Cp*Ru(NO)Me_2 (**1**) (1.48 g, 5.0 mmol) was added dropwise 0.45 mL (5.1 mmol) of HOTf in 10 mL CH_2Cl_2. The solution was stirred for 0.5 h followed by solvent removal *in vacuo*. The resulting solid was then dissolved in 40 mL of Et_2O and filtered into a fresh Schlenk tube. Hexane (20 mL) was added and the volume reduced *in vacuo* to 10 mL. The supernatant was decanted away and the resulting precipitate dried *in vacuo* to give 1.89 g (4.4 mmol, 88%) of a brown microcrystalline powder: mp 97–100 °C; IR (CH_2Cl_2) ν_{NO} 1787 cm^{-1}, (THF) ν_{NO} 1791 cm^{-1}; MS (EI) $[M]^+$ *m/e* 430 (4%), $[M-CH_3]^+$ *m/e* 415 (18%), [Cp*Ru(OTf)]+ *m/e* 385 (55%), $[Cp^*Ru(NO)=CH_2]^+$ *m/e* 280 (3.5%), $[HOTf]^+$ *m/e* 150 (73%), $[Cp^*]^+$ *m/e* 135 (100%); ^1H NMR ($CDCl_3$) δ 1.77 (s, 15H, C_5Me_5), 1.44 (s, 3H, Me); $^{13}C\{^1H\}$ NMR ($CDCl_3$) δ 8.3 (Me), 9.4 (C_5Me_5), 107.4 (C_5Me_5), 118.9 (q, $^1J_{CF}$ = 318 Hz, CF_3SO_3); $^{19}F\{^1H\}$ NMR (CH_2Cl_2) δ −76.5 (CF_3SO_3). Anal. Calcd for $C_{12}H_{18}NF_3O_4SRu$: C, 33.48; H, 4.22; N, 3.26. Found: C, 33.31; H, 4.29; N, 3.24.

Synthesis of Cp*Ru(NO)(C_6H_5)(OTf) (5). This complex was prepared in a manner analogous to that of Cp*Ru(NO)(CH_3)(OTf), starting from Cp*Ru(NO)$(Ph)_2$ (**2**) (1.39 g, 3.3 mmol) in 100 mL of CH_2Cl_2. The

(36) Hubbard, J. L.; Morneau, A.; Burns, R. M.; Zoch, C. R. *J. Am. Chem. Soc.* **1991**, *113*, 9176.

product was recrystallized from CH_2Cl_2 layered with hexane at –40 °C to afford 0.57 g (1.0 mmol 32%) of dark red-brown crystals; mp 102–105 °C; MS (EI) $[M]^+$ *m/e* 493 (4%), $[M-NO]^+$ *m/e* 463 (13%), [Cp*Ru(NO)(OTf)]$^+$ *m/e* 385 (9%), [Cp*Ru(OTf)]$^+$ *m/e* 327 (19%), $[Ph]^+$ *m/e* 77 (100%); IR (CH_2Cl_2) ν_{NO} 1799 cm^{-1}; ^{1}H NMR ($CDCl_3$) δ 1.72 (s, 15H, C_5Me_5), 7.10–7.20 (m, 5H, Ph); $^{13}C\{^1H\}$ NMR ($CDCl_3$) δ 9.0 (C_5Me_5), 110.3 (C_5Me_5), 120.3 (q, $^1J_{CF}$ = 320 Hz, CF_3SO_3), 125.5 (*p*-C_6H_5), 126.1 (*m*-C_6H_5), 128.1 (*o*-C_6H_5), 137.5 (*ipso*-C_6H_5); $^{19}F\{^1H\}$ NMR (CH_2Cl_2) δ –76.4 (CF_3SO_3). Anal. Calcd for $C_{17}H_{20}NO_4SF_3Ru$: C, 41.46; H, 4.09; N, 2.84. Found: C, 41.35; H, 4.15; N, 2.84.

Synthesis of Cp*Ru(NO)(*p*-tolyl)(OTf) (6). To a stirred solution of Cp*Ru(NO)(*p*-tolyl)$_2$ (**3**) (0.52 g, 1.15 mmol) in 50 mL of Et_2O was added 76 μL (0.05 mmol) of HOTf in 5 mL of Et_2O. The solution was stirred for 10 min. After solvent removal *in vacuo*, the residue was redissolved in 40 mL of Et_2O and filtered into a fresh Schlenk tube. The solution was concentrated to 15 mL *in vacuo*, layered with pentane (20 mL), and placed at –40 °C for 48 h, yielding 0.21 g (0.42 mmol, 36%) of a red-brown powder: mp 81–82 °C; IR (CH_2Cl_2) ν_{NO} 1797 cm^{-1}; ^{1}H NMR ($CDCl_3$) δ 1.72 (s, 15H, C_5Me_5), 2.30 (s, 3H, $C_6H_4CH_3$), 6.96 (dd, $^3J_{HH}$ = 8 Hz, 4H, C_6H_4); $^{13}C\{^1H\}$ NMR ($CDCl_3$) δ 9.73 (C_5Me_5), 20.8 (CH_3), 109.4 (C_5Me_5), 118.8 (q, $^1J_{CF}$ = 319 Hz, $CF_3SO_3^-$), 129.6 (*m*-$C_6H_4CH_3$), 134.8 (*p*-$C_6H_4CH_3$), 135.9 (*o*-$C_6H_4CH_3$), 149.2 (*ipso*-$C_6H_4CH_3$). Anal. Calcd for $C_{18}H_{22}NO_4SF_3Ru$: C, 42.68; H, 4.38; N, 2.77. Found: C, 42.50; H, 4.41; N, 2.70.

Characterization of Complex 7. Complex **1** (2.48 g, 8.37 mmol) was dissolved in 80 mL of CH_2Cl_2. To this solution was added dropwise excess triflic acid (1.60 mL, 18.08 mmol, 2.16 equiv) in 10 mL of CH_2Cl_2. The solution changed from deep red to purple with gas evolution. After 1 hour of vigorous stirring, the solution volume was reduced to ca. 10 mL and 60 mL of Et_2O was added to precipitate the product. The colorless supernatant solution was decanted away and the product dried under vacuum, yielding 4.68 g (8.29 mmol, 99%) of **7** as a purple microcrystalline powder: mp 209–211 °C; ^{1}H NMR (CD_2Cl_2) δ 1.87 (s, Cp*); $^{13}C\{^1H\}$ NMR (CD_2Cl_2) δ 10.1 (C_5Me_5), 113.9 (C_5Me_5), 119.4 (q, OSO_2CF_3, $^1J_{C-F}$ = 318.4 Hz); $^{19}F\{^1H\}$ NMR (CH_2Cl_2) δ –76.02; IR (CH_2Cl_2) ν_{NO} 1848 cm^{-1}. Anal. Calcd for $C_{12}H_{15}F_6NO_7RuS_2$ (564.4): C, 25.53; H, 2.68; N, 2.48. Found: C, 25.05; H, 2.75; N, 2.43.

Synthesis of Cp*Ru(NO)(C(Ph)=C(CH$_3$)C$_6$H$_4$) (8). A Schlenk tube was charged with 0.138 g (0.32 mmol) of Cp*Ru(NO)(CH_3)(OTf) (**4**), 0.057 g (0.32 mmol) of PhC≡CPh, and 10 mL of CH_2Cl_2. To the solution was added 120 μL (0.35 mmol) of *N*,*N*-diisobutyl-2,4-dimethyl-3-pentylamine, and the mixture was stirred at room temperature for 15 h. After removal of solvent *in vacuo*, the residue was extracted with 2 × 10 mL portions of hexane. The filtered extract was concentrated to 5 mL and placed at –40 °C for 24 h. The supernatant was decanted and the resulting solid dried under vacuum to yield 0.10 g (0.22 mmol, 68%) of orange microcrystals, mp 233–235 °C. X-ray quality crystals were grown from the slow evaporation of a hexane solution: MS (EI) $[M]^+$ *m/e* 459 (97%), $[M-NO]^+$ *m/e* 428 (100%), $[Cp^*Ru]^+$ *m/e* 236 (45%); IR (CH_2Cl_2) ν_{NO} 1738 cm^{-1}; ^{1}H NMR ($CDCl_3$) δ 1.52 (s, 15H, C_5Me_5), 2.12 (s, 3H, Me), 6.9–7.4 (m, 9H, phenyls); $^{13}C\{^1H\}$ ($CDCl_3$) δ 9.6 (C_5Me_5), 15.6 (Me), 104.1 (C_5Me_5), 122.0, 123.5, 124.7, 128.4, 137.2, 145.0, 161.0, 168.4 (Ph's and C=C). Anal. Calcd for $C_{25}H_{27}NORu$: C, 65.48; H, 5.93; N 3.05. Found: C, 65.24; H, 6.01; N, 3.02.

Synthesis of Cp*Ru(NO)(C(Ph)=C(Ph)C$_6$H$_4$) (9). A Schlenk tube was charged with 0.12 g (0.24 mmol) of Cp*Ru(NO)(C_6H_5)(OTf) (**5**), 0.043 g (0.24 mmol) of PhC≡CPh, and 20 mL of CH_2Cl_2, and the mixture was stirred magnetically for 10 h at room temperature. After solvent removal *in vacuo* the resulting solid was extracted with 20 mL of hexane. The hexane solution was evaporated to afford an orange solid. Recrystallization by slow evaporation of hexane gave 0.02 g (0.11 mmol, 46%) of red needles: mp 180 °C; MS (EI) $[M]^+$ *m/e* 521 (100%), $[M-NO]^+$ *m/e* 491 (33%); IR (CH_2Cl_2) ν_{NO} 1734 cm^{-1}; ^{1}H NMR ($CDCl_3$) δ 1.57 (C_5Me_5) 6.75–7.55 (m, Ph's); $^{13}C\{^1H\}$ NMR ($CDCl_3$) δ 9.6 (C_5Me_5), 104.3 (C_5Me_5), 123.5, 123.8, 124.5, 124.9, 125.8, 127.0, 128.3, 128.8, 131.6, 137.5, 140.6, 147.3, 153.4, 161.0, 168.4, 171.6.

Cp*Ru(NO)(C(Ph)=C(Ph)C$_6$H$_3$CH$_3$) (10). This complex was prepared starting from 0.2 g (0.4 mmol) of Cp*Ru(NO)(*p*-tolyl)(OTf) (**6**) and 0.11 g (0.62 mmol) of PhC≡CPh in 20 mL of CH_2Cl_2. The solution was stirred for 12 h at room temperature. After solvent removal *in vacuo*, the residue was extracted with 3 × 10 mL portions of hexane. Solvent removal *in vacuo* followed by sublimation to remove the unreacted PhC≡CPh and recrystallization from evaporation of hexane gave 0.1 g (0.2 mmol, 47%) of red crystals: mp 222 °C; MS (EI) $[M]^+$ *m/e* 534 (100%), $[M-NO]^+$ *m/e* 504 (80%); IR (CH_2Cl_2) ν_{NO} 1736 cm^{-1}; ^{1}H NMR ($CDCl_3$) δ 1.57 (s, 15H, C_5Me_5), 2.30 ($C_6H_3CH_3$), 6.67 (d, 1H, $^3J_{HH}$ = 7.6 Hz), 6.76 (br d, 1H, $^3J_{HH}$ = 7.6 Hz ($^4J_{HH}$ = 1.5 Hz from decoupling at δ 2.3)), 6.87–7.2 (m, 10H, phenyl rings), 7.29 (br s, 1H, $^4J_{HH}$ = 1.5 Hz from decoupling at δ 2.3); $^{13}C\{^1H\}$ ($CDCl_3$) δ 9.7 (C_5Me_5), 21.2 ($C_6H_3CH_3$), 104.2 (C_5Me_5), 123.4, 124.3, 125.5, 125.7, 126.9, 128.9, 132.7, 138.6, 140.8, 147.4, 153.2, 158.1, 168.3, 170.0 (Ph's and C=C). Anal. Calcd for $C_{31}H_{31}NORu$: C, 69.64; H, 5.84; N, 2.62. Found: C, 69.43; H, 5.82; N, 2.57.

Reaction Profiles by NMR Spectroscopy. In a typical experiment an NMR tube was loaded with 7 mg of **4** or **5** and 10 equiv of PhC≡CPh, 0.5 mL of $CDCl_3$ was added along with 1 μL of 1,2-dichloroethane as an internal standard for ^{1}H NMR spectroscopy, and a ^{1}H NMR spectrum was taken immediately. The reaction was then followed by both ^{19}F and ^{1}H NMR spectroscopy over a period of 30 h.

Equilibrium Measurements in THF. An NMR tube was charged with 8 mg of **5** and 0.5 mL of freshly distilled THF, and a similar NMR tube containing 7 mg of **4** was also prepared. ^{19}F NMR spectra were measured over a range of 22–55 °C. The solution was allowed to equilibrate in the probe of the NMR spectrometer at the desired temperature before a spectrum was measured. Long T_1 delays were routinely employed so that the integration values from the spectra could be used for subsequent van't Hoff plots.

Reaction of 8 with 1 equiv of HOTf. An NMR tube was loaded with 4 mg of **8** and 0.5 mL of $CDCl_3$ and stoppered with a rubber septum. An initial ^{1}H NMR spectrum was measured. Using a microliter syringe, 0.5 μL of HOTf was added through the septum, and a spectrum measured. The solvent was removed *in vacuo* and CH_2Cl_2 added. A small amount of the solution was removed and used to obtain an IR spectrum. The solvent was again removed *in vacuo*, the resulting solid dissolved in $CDCl_3$, and a ^{1}H NMR spectrum remeasured.

Preparation of DOTF. A vacuum bulb was charged with 6 mL of Tf_2O (triflic anhydride) and 0.5 mL of D_2O and stirred for several hours. The resulting solution was distilled under vacuum to remove unreacted D_2O and Tf_2O. The enrichment as DOTf was determined to be >90% by assessing the CH_4:CH_3D ratio produced when Cp*Ru(NO)(Me)$_2$ (**1**) is treated with the prepared DOTf.

Reaction of 8 with DOTf. An NMR tube was loaded with 6 mg of **8**, dissolved in 0.5 mL of CH_2Cl_2, and stoppered with a rubber septum and a ^{2}H NMR spectrum recorded. A microliter syringe was used to deliver 1 μL of DOTf through the septum and a ^{2}H NMR spectrum measured.

Reaction of 8 with Excess HOTf. An NMR tube was loaded with 3 mg of **8** and 0.5 mL of $CDCl_3$ and stoppered with a rubber septum. An initial ^{1}H NMR spectrum was measured. A microliter syringe was used to deliver 5 μL of HOTf through the septum, and a spectrum was measured.

Acknowledgment. The support of the National Science Foundation (Grant CHE-9215872) is gratefully acknowledged. We acknowledge the NSF (Grant CHE-9002379) and the Utah State University Research Office for jointly funding the purchase of the X-ray diffractometer. R.M.B. thanks Utah State University for a USU Presidential Fellowship for 1992–93 and Dr. C. R. Zoch for assistance in the initial characterization of complex **7**.

Supplementary Material Available: Tables giving complete details of the X-ray data collection and refinement and complete lists of bond angles, bond distances, final anisotropic thermal parameters, calculated H atom coordinates, and atomic coordinates and equivalent isotropic thermal parameters for Cp*Ru(NO)(Ph)(OTf) (**5**), Cp*Ru(NO)(C(Ph)=C(Me)C$_6$H$_4$) (**8**), and Cp*Ru(NO)(C(Ph)=C(Ph)C$_6$H$_3$CH$_3$) (**10**) (21 pages); tables of observed and calculated structure factors for **5**, **8**, and **10** (42 pages). This material is contained in many libraries on microfiche, immediately follows this article in the microfilm version of the journal, and can be ordered from the ACS; see any current masthead page for ordering information.